

**A comparison of concentrations of macronutrients and chlorophyll a in high- and
low- chlorophyll concentration areas around the Galápagos Islands**

Running head: Nutrient concentrations in the Galápagos

Tamra Dickson

2 March 2006

University of Washington
School of Oceanography
Box 357940
Seattle, Washington 98195-7940

Acknowledgements

I would like to acknowledge Professors Roy Carpenter, Mark Holmes, Seelye Martin and Gabrielle Rocap for their amazing knowledge, helpfulness and never-ending patience. I also want to thank teaching assistant Llyd Wells, for his countless hours of dedication and putting up with our endless questions and complaints. In addition, I thank the rest of the “team” of University of Washington’s spring 2006 Ocean 444 class; because working together was the only way we could pull this whole caper off. Finally I thank Mary Marsh, Mike Town, Peter Saxby, Kirby Zornes, Neil Biermann, Kate Allender, Carol Berg, Carol Burton, Mike Hansen, Rick Keil, Mitsuhiro Kawase, Paul Quay and Richard Sternberg for teaching me the science that got me this far and keeping me motivated. This work was supported by the University of Washington and outside private donors.

Non-Technical Summary

By understanding nutrient levels around the islands as well as physical process that affect those levels, we can better understand food webs involving phytoplankton and zooplankton abundance, fish abundance and distributions of marine mammals. Leg 2 of R/V Thomas G. Thompson cruise 189 took place in the Galápagos archipelago off the coast of Ecuador from 20 to 28 January 2006. Water samples to measure nutrient concentrations were taken at six stations, three of them in the west (Bio-1, Bio-2 and Bio-3) and three of them in the east (Bio-1, Bio-2 and Bio-3) of the main island of Isabela. Samples to the west had higher chlorophyll concentration than those in the east, as seen both from collected samples and in satellite imagery taken of chlorophyll concentration the same week as the cruise. It was also determined to be a “normal” non-El Niño year with upwelling in the western part of the archipelago. All nutrient concentrations measured (NH_4^+ , NO_3^- , PO_4^{3-} , and Si) increased with depth. Nitrate concentrations were higher in high chlorophyll concentration areas than areas with low chlorophyll while silica was lower in high chlorophyll areas. This was likely because larger diatoms, which take up more silica, dominated the western stations. Ammonium concentrations were low all around the island as expect, since it is thermally unstable and preferred for use by phytoplankton in photosynthesis. Phosphate was distinctly higher in stations Bio-1, Bio-3 and Bio-6 than in Bio-2, Bio-4, and Bio-6, but the split was between west/east of inshore/offshore. It may be because of upwelling of colder, nutrient rich waters or because of terrestrial inputs. Measurements of these four macronutrient concentrations around the Galápagos Islands help to understand nutrient cycling in the area as well as variations in micro flora and fauna size in different locations in the archipelago.

Abstract

The Galápagos archipelago is a hot spot of life in an open ocean of low production. The ecosystem of the islands depends on dissolved nutrients, which determine how much and what types of phytoplankton occur. This then determines size and distribution of micro and macro fauna that feed in the nutrient-rich waters. On R/V Thompson G. Thompson cruise 189 from 20 to 28 January 2006, waters west of Isla Isabela were colder and had higher nutrient and chlorophyll concentration than waters east of Isabela. These results were confirmed by satellite images of sea surface chlorophyll concentrations taken the week of the cruise. It was also determined to be a “normal” non-El Niño year with upwelling in the western part of the archipelago (compared to upwelling in the western part of the archipelago during El Niño years). All measured nutrient concentrations increased with depth. Nitrate concentrations (between $15 \mu\text{mol L}^{-1}$ and $25 \mu\text{mol L}^{-1}$) were higher in high chlorophyll concentration areas to the west than low concentration areas to the east. Silica was the opposite with concentrations (between 1.0 and $5.0 \mu\text{mol L}^{-1}$) being generally higher in the eastern stations. This was likely due to fewer and smaller diatoms not using as much silica. Ammonium was below $1.0 \mu\text{mol L}^{-1}$ for all stations because it is preferred more than nitrate and takes less energy and dissolved iron to be used. Phosphate (1 to $5 \mu\text{mol L}^{-1}$) was higher at stations closer to shore than further offshore. Measurements of macronutrient concentrations around the Galápagos Islands help to understand nutrient cycling as well as variations in micro flora and fauna size in different locations in the archipelago.

Introduction

For centuries, sailors and scientists alike have marveled at the uniqueness that is the Galápagos Islands. They called them “Las Islas Encantadas” (The Enchanted Isles) for their ability to appear and disappear into the cloudbanks that shrouded the volcanoes that created them. The islands were said to be the home of bizarre and wondrous creatures. A unique feature of the Galápagos fauna is the absence of large native land mammals due to all native species arriving there originally by either wind or currents. The land animals are fantastically divergent from mainland species, but it is the surrounding marine reserve that is the real ecological paradise. The 140,000 square kilometers of ocean within the Galápagos Marine Reserve (as compared to a land area of 8,000 km², 97% of which comprises the Galápagos National Park) are home to hundreds of animal species who depend on the sea for their food. Contributing to this is the convergence of several currents around the archipelago and the physical and chemical properties of the water these animals inhabit that provide a rich marine food web well worthy of study.

The Galápagos archipelago ecosystem is affected by several different subsurface and surface level currents (Fig. 1). The South Equatorial Current (SEC) is fed by the Peru and Panama Current Systems and runs along the equator through the Galapagos. It is not clear what the exact path of the SEC current is, but a general trend of running north of San Cristobal Island and between San Salvador and Genovesa Islands is believed to be roughly the location, with some variability from year to year (Steger et al. 1998).

In normal or “Non El Niño” years, the EUC hits the archipelago shelf from the west and upwells to the surface (Fig. 1) offshore of Isla Isabela and Fernandina, bringing

cold, nutrient rich water from the depths. These waters are high in macronutrients such as nitrate (NO_3^-), phosphate (PO_4^{3-}) and silica (Si) that phytoplankton need for growth (Lindley and Barber 1998). In the Galapagos, there is a general trend of high chlorophyll concentrations west of Isabela and lower concentrations in the central and eastern areas of the archipelago where the EUC flow is obstructed (Fig 2). The EUC is also rich in iron, another macronutrient needed for growth by most organisms, and yet production is limited in many areas of the Galapagos and surrounding waters (Houvenaghel 1984). This could be because iron is unstable and is readily oxidized from a usable form to an unusable form.

In non-normal El Niño years, the EUC flows in the opposite direction, upwelling in the eastern part of the archipelago. Nutrient levels in the main archipelago are not replenished and primary production and chlorophyll concentration levels decrease dramatically. This prevents macro fauna from being able to feed closer to the islands and causes a crash throughout the entire marine ecosystem, especially in species that nest on land but feed out at sea (Cooper and Laurie 1987, Vargas et al. 2006).

Areas that are low in productivity despite high nutrient concentrations are referred to as High Nutrient-Low Chlorophyll or HNLC areas (Fig 3). HNLC regions of open oceans could be because some nutrients are limiting in the open ocean (Martin et al. 1994). While iron itself is not limiting in these areas, phytoplankton can only use Fe^{2+} , and most iron in the ocean oxidizes quickly into the unusable form of Fe^{3+} (Lindley and Barber 1998). The IronEx and PlumEx experiment tested the possibility of iron being a limiting nutrient (Martin et al. 1994, Sakamoto et al. 1998) and was further explored in other iron-enrichment experiments in other HNLC regions of the world (Coale et al.

2004). Measurement of dissolved iron concentrations are very hard to do, however, since it requires equipment and lab analysis methods to be trace metal-free.

During the IronEx experiment (Martin et al. 1994, Lindley and Barber 1998) in which a patch of the Equatorial Pacific was deliberately enriched with iron, scientists typically found chlorophyll concentrations at a maximum 20 to 30 m below the surface in iron enriched waters. This would give support to the idea that the chlorophyll maximum is not always on the surface and thus depends on some factor aside from incoming sunlight. This factor may be the aforementioned availability or lack of availability of nutrients. The PlumEx experiment, which was the second leg of the IronEx experiment and was conducted closer to the Galápagos (Sakamoto et al. 1998), showed a definite trend of higher dissolved macronutrient concentrations toward the west side of the Galápagos archipelago as compared to lower concentrations toward the east. This would support the increased surface chlorophyll concentrations found in satellite images on the western side as seen by Feldman et al. (1984, Fig. 4) and Feldman (1986, and 2). The northern waters are also fresher and warmer overall than that of the southern waters (Sakamoto et al. 1998, Steger et al. 1998). Partial CO₂ concentrations (pCO₂) and Total CO₂ (TCO₂) levels were higher in the west, which was interesting considering that higher chlorophyll should mean less carbon available in the system if temperatures are the same because productivity significantly depletes TCO₂ (Sakamoto et al. 1998).

Ammonium and nitrate are the two most commonly used forms of nitrogen in the ocean. Most phytoplankton prefer to use ammonium because it is already reduced and is thus more easily assimilated. Nitrate is used in the absence of ammonium despite the need for more energy to reduce it for incorporation into amino acids. Other important

nutrients are phosphate and silica. Phosphate is essential for life processes as phytoplankton use it for building ATP, the molecule that stores energy as well as the backbone of DNA and RNA chains. In contrast to other nutrients, only some phytoplankton use silica.

During El Niño in the Galápagos, nutrient concentrations are lower and red and brown algae can replace edible green algae as the primary plants. Up to 90% of offspring of iguana, penguin, sea lion, and others die in their first year during El Niño years (Cooper and Laurie 1987, Trillmich and Kooyman 2001, Vargas et al. 2006). An excess of macronutrients can also be detrimental. Too high a concentration of nitrate or phosphate can create harmful algal blooms that deplete oxygen levels and cause anoxic conditions that kill fish and other marine life (Sakamoto et al. 1998).

The Ecuadorian government limits the amount of research cruises to the Galapagos, and so most chlorophyll and primary production data are inferred from satellite photo images (Fig 2., Feldman 1986). These images read mainly the chlorophyll levels on the sea surface, so it may be possible that chlorophyll concentration data obtained in this way underestimate or miss the subsurface chlorophyll maximum entirely and significantly underestimate primary productivity. It is also important to determine the vertical profile of chlorophyll concentrations to understand better how chlorophyll concentrations relate to nutrient concentrations.

On Leg 2 of TN 189 cruise from 20 to 28 January 2006, I measured for the concentrations of four main macronutrients -- ammonium, nitrate, phosphate, and silica -- at six stations around the western islands of the Galapagos (Fig. 5). Satellite pictures showed a verification of “normal” non-El Niño conditions (Fig. 6).

I determined whether a positive relationship existed between measured macronutrient concentrations and concentrations of chlorophyll gathered by other students. I hypothesized that stations predicted to have similar productivity would show similar concentration levels of macronutrients and chlorophyll. I also expected to see nutrients and salinity increase with depth while dissolved oxygen and temperature decrease as seen in previous studies by Richards and Broenkow (1969) and Cline and Richards (1972). Lastly, I examined other nutrient ratios to see if they accorded with expected Redfield stoichiometry (an N:P ratio of 16:1). Comparisons between levels of chlorophyll at the chlorophyll maximum and at the surface may improve interpretation of satellite-based estimates of phytoplankton concentration and primary production in the Galapagos archipelago.

Shipboard sampling and analytical methods

Stations were chosen based on satellite photos from Feldman (1986) showing areas of high and low surface chlorophyll concentration (Fig. 2) and to coordinate with other student's projects. All water samples were taken using a 24-bottle CTD (conductivity, temperature, depth) rosette with sensors for measuring in-situ temperature, salinity (measured by conductivity), chlorophyll fluorescence, percent light transmission, photosynthetically active radiation (PAR), dissolved oxygen concentration, and depth (calculated from pressure). Water was sampled at five depths from six stations (Table 1, Fig. 5), with Bio-1, Bio-2 and Bio-3 being west of Isla Isabela and Bio-4, Bio-5 and Bio-6 being east of Isla Isabela. The five depths differed at each station because they were picked to be at the 100% light level, chlorophyll maximum, 50% light level, chlorophyll minimum, and 1% light level, which were different at each station. Depths for the

chlorophyll maximum and minimum were decided from the live readings taken by the chlorophyll fluorescence sensor on the CTD. 100%, 50% and 1% light levels depths were decided from the live readings taken by the PAR sensor on the CTD.

Phosphate and silica analysis

Phosphate was measured using a standard procedure set forth by Grasshoff et al. (1983). Silica was measured using a standard procedure set forth by Strickland and Parsons (1968). Both involved the use of chemical reagents to produce a color change in the water, with darker samples having higher concentrations. I measured absorbance with the use of a spectrophotometer. All plastic sample bottles were acid-cleaned, rinsed three times with distilled water and once with the sample seawater before being filled with approximately 60 ml of sample water (Strickland and Parsons 1968, Grasshoff et al. 1983).

Before the phosphate analysis, I calibrated the spectrophotometer each day with fresh standards (0.0, 0.5, 1.0, 2.0, and 3.0 $\mu\text{mol L}^{-1}$) made from dry potassium dihydrogen phosphate (KH_2PO_4). The working reagent and ascorbic acid were added to the sample, mixed thoroughly, and allowed to stand for 15-30 minutes until a blue color fully developed (color is stable for testing for several hours after this). Once absorption of blanks and standards were measured at a wavelength of 810 nm, samples were analyzed (Grasshoff et al. 1983) using the equation of the standard curve to get concentrations from absorbance levels.

Silica analysis was very similar to the phosphate analysis except for the use of concentrations of 6, 12, 24, 36, 48, and 60 $\mu\text{mol L}^{-1}$ primary silica standards and a reducing agent of metol-sulphite solution with oxalic acid solution. The samples were

also shaken and read on a spectrophotometer at a wavelength of 885 nm after blanks and standards were measured to calibrate the machine (Strickland and Parsons 1968). A standard curve was also used to translate absorbance readings into concentrations.

Data obtained from other students

Ben Gilmore measured primary productivity using incubation experiments to get a change in dissolved oxygen and dissolved organic carbon. Oxygen concentrations were determined by using a titration method described by Carpenter (1965). Tasha Snow measured chlorophyll concentration using the procedure described by Holm-Hansen and Riemann (1978). Joni Werdeman measured dissolved concentrations of ammonium using procedures described by Holmes et al. (1999) and dissolved nitrate using procedures described by UNESCO (1994).

Results

All stations showed subsurface nutrient profile maximas. For ammonium, nitrate and silica, western stations Bio-1, Bio-2 and Bio-3 had lower concentrations than eastern stations Bio-4, Bio-5 and Bio-6 at the surface. Below the mixed layer, western stations had higher concentrations compared to eastern stations (Fig. 7B). Phosphate was interesting in that Bio-1, Bio-3 and Bio-6 were higher than Bio-2, Bio-4 and Bio-5 throughout the whole water column (Fig. 8A). In addition, there is a general trend of nitrate having the highest concentration at each station followed by silica, then phosphate, and ammonium being least abundant for most depths with some variability at surface and deep stations.

The nutrient profiles for western stations Bio-1, Bio-2 and Bio-3, which were seen to be in high chlorophyll concentration areas (Figs. 9A, 10A, 11A), showed high

concentrations of nitrate below the mixed layer (20 to 25 $\mu\text{mol L}^{-1}$), medium concentrations of silica (7 to 15 $\mu\text{mol L}^{-1}$) and low concentrations of ammonium (less than 2 $\mu\text{mol L}^{-1}$ for all samples). Phosphate had medium concentrations below the mixed layer for Bio-1 and Bio-3 (4-8 $\mu\text{mol L}^{-1}$) but low concentrations for Bio-2 (1-2 $\mu\text{mol L}^{-1}$). Dominant changes in seawater properties (temperature, salinity) occurred at the same depth as a steep increase in macronutrients (Figs. 9A, 10A, 11A) and a steep decrease in dissolved oxygen and chlorophyll concentrations (Figs. 9B, 10B, 11B).

In the mixed layer, western stations Bio-1, Bio-2 and Bio-3 had medium nitrate concentrations (5 to 10 $\mu\text{mol L}^{-1}$), low silica concentrations (1-5 $\mu\text{mol L}^{-1}$) and very low ammonium concentrations (less than 2 $\mu\text{mol L}^{-1}$). Phosphate concentrations at Bio-1 and Bio-3 were between 2 and 6 $\mu\text{mol L}^{-1}$. The phosphate concentrations at Bio-2 were between 0.5 and 2 $\mu\text{mol L}^{-1}$ (Figs. 9A, 10A, 11A).

The eastern stations Bio-4, Bio-5 and Bio-6, which were predicted to be in low chlorophyll concentration areas (Figs. 12A, 13A, 14A), showed slightly lower subsurface concentrations in nitrate (10-20 $\mu\text{mol L}^{-1}$). Silica concentrations were higher below the mixed layer (12-17 $\mu\text{mol L}^{-1}$). (Fig. 8B). This could be because the west side of Isabela is dominated by silica-containing diatoms that are taking up more silica than the phytoplankton on the east side (Table 2, Snow 2006). The ammonium levels only about 0.1 or 0.2 $\mu\text{mol L}^{-1}$ lower in eastern stations than in western stations (Fig. 7A).

Eastern stations had lower nitrate in the mixed layer (between 5 and 10 $\mu\text{mol L}^{-1}$). Silica in the east was higher in the mixed layer than in the west at 2 to 7 $\mu\text{mol L}^{-1}$. Ammonium was very low, but still measurably lower than in the west (0.25 to 0.75 $\mu\text{mol L}^{-1}$). Phosphate at Bio-4 and Bio5 was around 0.5 $\mu\text{mol L}^{-1}$ and between 2 and 3 $\mu\text{mol L}^{-1}$.

¹ at Bio-6 (Fig. 8). Dominant changes in seawater properties (temperature, salinity) also occurred at the same depth as a steep increase in macronutrients (Figs. 12A, 13A, 14A) and a steep decrease in dissolved oxygen and chlorophyll concentrations (Figs. 12B, 13B, 14B).

Bio-2 is the station that had duplicates of phosphate and silica run. Each depth was averaged depth profile. Error from each depth was averaged to get an error for the whole data set (Fig. 10A). Phosphate had a standard error of $0.38 \mu\text{mol L}^{-1}$. Silica had a standard error of $0.53 \mu\text{mol L}^{-1}$.

It should be noted that station Bio-6 had no surface sample taken due to equipment failure. In addition, the surface sample of Bio-1 showed a negative silica concentration (Fig. 9B). Allowing for error, this would mean that the concentration was at levels that are not reliably high enough to be measured by the procedure used.

Discussion

The western side of Isabela predicted to be of high chlorophyll concentration than the eastern side (Feldman 1986, Fig. 2) was still that way when we took our cruise (Fig. 6). All our ammonium measurements were too similar to discern trends by station with the exception of the samples from station Bio-2. This could be because Bio-2 is on the west side of Isla Isabela in Elizabeth Bay. A large part of the coastline of Isabela is believed to be a site of upwelling of the EUC (Houvenahgel 1984). Bio-2 is near land and the middle of the believed path of the EUC.

Nitrate was higher at the higher chlorophyll concentration near the surface at Bio-1, Bio-2 and Bio-3 possibly because of grazers exhibiting “sloppy feeding” and bacteria adding atmospheric inputs. In order to know for sure, one would have to study how

much of the nutrients were lost at each trophic food web level and what other nitrogen species were present in the water column. The west had lower subsurface nitrate compared to the east and stations Bio-1 and Bio-3 exhibited much lower nitrate concentrations nitrate at the lowest depths than in the east. The fact that the west has higher concentrations at the surface and lower at the subsurface could be due to the fact that the waters of the western and eastern sides of the island are two distinct water masses. In addition, the main source of nitrate input may be different on one side of the island than on the other. There are no data from Bio-2 past 100 m, but it is expected that there would be a drop in nutrient concentration as seen in Bio-1 and Bio-3 (Figs. 9A, 10A, 11A). Nitrate numbers also resembled those in previous studies done by Richards and Broenkow (1969) and Cline and Richards (1972) with maximum concentrations being below the surface as was expected.

Phosphate is clearly divisive with Bio-1, Bio-3, and Bio-6 having concentrations higher by around $2.0 \mu\text{mol L}^{-1}$ than Bio-2, Bio-4, and Bio-5. This division was not by western and eastern stations nor was it by inshore and off shore stations. The cause of this division is unknown. It is likely, however, that phosphate is not the only nutrient attributing to the increased amount of western chlorophyll concentration in that nitrate was also higher there in the upper photic zone (0-20 m) than it was in the eastern. It is most important what concentrations are in the photic zone of the upper 40 m because chlorophyll is virtually nonexistent where light does not reach (Feldman 1986). A Redfield ration of 16:1 for N:P was not observed; in fact, the number was closer to 4:1 (Fig. 15). This could be due to phosphate being in overabundance because of the proximity to coastlines.

Silica stands alone because not all phytoplankton need it, only those who build silica-based shells. Other students observed that the western side was dominated by >20 μm phytoplankton and the eastern side is dominated by <2.0 μm phytoplankton (Table 2, Snow 2006). Chain-forming diatoms that use silica to build their shells are large and were found to be dominant in the west. Since they took up a lot of silica, this would explain why there are lower concentrations of silica in the west when compared to the eastern stations, especially on the western side of Isabela where the chlorophyll maximum was consistently found to be at the surface (Table 2). In addition, silica is added into the water by hydrothermal venting and there could be more volcanic activity in the east at depth leading to more silica in the subsurface water (Houvenahgel 1984).

Zooplankton was measured with three mesh nets of sizes 102-209 μm , 209-333 μm and >333 μm . The zooplankton generally followed the trend of phytoplankton size with greater than 333 μm being dominant at the western stations Bio-1, Bio-2 and Bio-3 (Table 2, Geri 2006) and smaller <333 μm being dominant at the eastern stations Bio-4, and Bio-6 (Table 2, Geri 2006). This would be expected since smaller zooplankton often prefer smaller phytoplankton and would thus be not as common in an ecosystem dominated by larger phytoplankton. Station Bio-5 was the differing station in that zooplankton of greater than 333 μm were seen despite the fact that <2 μm phytoplankton were dominant (Geri 2006). It could be that the zooplankton at this station had just adapted to eating smaller phytoplankton than they would elsewhere or were eating other zooplankton. This is ecologically important because the large marine animals depend on zooplankton for food and without phytoplankton and zooplankton, the whole ecosystem would crash.

Primary production was highest at western surface stations. Below the surface, production levels were generally similar in both west and east sides of Isabela (Table 2, Gilmore 2006). The variations could be because stations Bio-2, Bio-4 and Bio-6 were taken at night. Though chlorophyll concentration would remain constant during a 24-hour period, photosynthetic reactions and sugar formation would halt during the night because of the absence of sunlight.

Water was taken at Bio-2, Bio-4 and Bio-6 for Iron-added growth rate experiments. Bio-2 showed no effect of added iron on growth rates which can be expected given that phytoplankton concentration is already high in that area (Table 2, Guo 2006). Bio-4 showed an increase in growth rates compared to the control sample but it was the slowest growth rate overall. Bio-6 showed no significant growth (Table 2, Guo 2006). It can be determined that iron fertilization only helps when chlorophyll concentration is lower to start with. It is important to know how iron concentration would effect growth because an increase in iron concentration could lead to an increase in primary productivity and create a sink for carbon (Martin et al. 1994 and Coale et al. 2004). However, since there was no way of measuring iron concentration directly, only the chlorophyll concentration, than there is no way to determine if addition of iron was the only thing affecting growth.

Conclusions

As was expected, a positive relationship existed in the photic zone between measured macronutrient concentrations and concentrations of chlorophyll gathered by other students. Below the photic zone, macronutrients concentration continued to increase as was predicted based on previous studies. Stations in the west generally

showed higher surface concentrations for all nutrients. Eastern stations had generally higher subsurface concentrations. Salinity also increased with depth while dissolved oxygen and temperature decreased. A Redfield ration of 16:1 (N:P) was not observed, in fact the number was closer to 3.5:1. Data still need to be collected from more stations further southeast and northeast in the archipelago in order to get a better picture of water. Samples must also be taken under both El Niño and non-El Niño conditions. Understanding of how nutrient concentrations vary with time will help us understand how to predict changes to phytoplankton and zooplankton abundance and how the larger marine animals will adapt accordingly.

References

- Carpenter, J.H. 1965. The Chesapeake Bay Institute technique for the Winkler dissolved oxygen method. *Limnol. Oceanogr.* **10**:141-143.
- Cline, J.D. and F.A. Richards. 1972. Oxygen Deficient Conditions and Nitrate Reduction in the Eastern Tropical North Pacific Ocean. *Limnol. Oceanogr.* **17**: 885-900.
- Coale, K.H. and 47 other authors. 2004. Southern Ocean Iron Enrichment Experiment: Carbon Cycling in High- and Low-Si Waters. *Science* **304**: 408-414.
- Cooper, J.E., W.A. Laurie. 1987. Investigation of deaths in marine iguanas (*Amblyrhynchus cristatus*) on Galapagos. *J. Comp. Pathol.* **2**: 129-136.
- Feldman, G., D. Clark, D. Halpern. 1984. Satellite Color Observations of the Phytoplankton Distribution in the Eastern Equatorial Pacific During the 1982-1983 El Niño. *Science* **226**:269-271.
- Feldman, G. 1986. Patterns of phytoplankton production around the Galapagos Islands, p. 77–106. *In*: M. J. Bowman, C. M. Yentsch and W. T. Peterson [eds.], *Tidal Mixing and Plankton Dynamics*. Springer-Verlag.
- Grasshoff, K., M. Ehrhardt, K. Kremling. 1983. *Methods of Seawater Analysis*, 2nd edition, Verlag Chemie pg. 125-131.
- Geri, K. 2006. Zooplankton community composition and size distribution in relation to phytoplankton in the Galápagos Islands. Unpublished Bachelor's Thesis, University of Washington.
- Gilmore, B. 2006. Primary production around the Galápagos Islands and the effect of cloud cover and differing light regimes. Unpublished Bachelor's Thesis, University of Washington.

- Guo, W. 2006. Inter-island comparison of phytoplankton growth rates and herbivory rates. Unpublished Bachelor's Thesis, University of Washington.
- Holm-Hansen, O. and B. Riemann. 1978. Chla determination: improvements in methodology. *Oikos* **30**: 438-447.
- Holmes, R., A. Aminot, R. Keroul, B. Hooker, B. Peterson. 1999. A simple and precise method for measuring ammonium in marine and freshwater ecosystems. *Can. J. Fish. Aquat. Sci.* **56** 1801-1808.
- Houvenahgel, G.T. 1984. Oceanographic conditions in the Galapagos Archipelago and their relationships with life on the Islands, p. 43-54. *In* R. Perry [ed.], *Key environments, Galapagos*. Pergamon Press.
- Lindley, S.T. and R.T. Barber. 1998. Phytoplankton response to natural and experimental iron addition. *Deep-Sea Res. Pt. II* **45**: 1135-1150.
- Martin, J. H. and 43 other authors. 1994. Testing the iron hypothesis in ecosystems of the equatorial Pacific Ocean. *Nature* **371**: 123-129.
- Richards, F.A. and W.W. Broenkow. 1969. Chemical Changes, Including Nitrate Reduction, in Darwin Bay, Galapagos Archipelago, Over a 2-Month Period, 1969. *Limnol. Oceanogr.* **16**: 758-765.
- Sakamoto, C.M., F.J. Millero, W. Yao, G.E. Friederic, F.P. Chavez. 1998. Surface seawater distributions of inorganic carbon and nutrients around the Galapagos Islands: results from the PlumEx experiment using automated chemical mapping. *Deep-Sea Res. Pt. II* **45**: 1055-1071.
- Snow, T. 2006. Composition and distribution of phytoplankton around the Galápagos Archipelago. Unpublished Bachelor's Thesis, University of Washington.

- Steger, J.M., C.A. Collins, P.C. Chu. 1998. Circulation in the Archipiélago de Colón (Galapagos Islands). *Deep-Sea Res. Pt. II* **45**: 1093-1114.
- Strickland, J.D.H., and Parsons, T.R. 1968. Determination of reactive silicate. In: *A Practical Handbook of Seawater Analysis*. Fisheries Research Board of Canada, Bulletin **167**: 65-70.
- Trillmich, F., and G.L. Kooyman. 2001. Field metabolic rate of lactating female Galapagos fur seals (*Arctocephalus galapagoensis*): the influence of offspring age and environment. *Comp. Biochem. Phys. A* **4**: 741-749.
- UNESCO. 1994. Protocols for the Joint Global Ocean Flux Study (JGOFS) core measurements. *IOC Manual and Guides*. **29**.
- Vargas, F.H., S. Harrison, S. Rea, D.W. MacDonald. 2006. Biological effects of El Niño on the Galapagos Penguin. *Biol. Conserv.* **1**: 107-114.

Table 1. Placement of sampling stations for biology and chemistry experiments on Thompson cruise 189.

Station	Latitude	Longitude	Day	Time (GMT)
Bio-1	S 0° 37.00'	W 91° 41.99'	1/21/2006	23:24
Bio-2	S 0° 37.01'	W 91° 29.00'	1/23/2006	08:05
Bio-3	S 0° 13.61'	W 91° 36.41'	1/22/2006	19:36
Bio-4	S 0° 01.00'	W 91° 07.99'	1/25/2006	08:51
Bio-5	S 0° 32.01'	W 90° 46.99'	1/24/2006	13:10
Bio-6	S 0° 55.01'	W 89° 59.96'	1/21/2006	08:25

Table 2. Station data from colleagues for surface and depth.

	Bio1	Bio2	Bio3	Bio4	Bio5	Bio6
	West Side	West Side	West Side	East Side	East Side	East Side
Primary Productivity ($\mu\text{mol L}^{-1} \text{d}^{-1}$ carbon) (Gilmore 2006).	Surf-30 Depth-5	Surf-10 Depth-7	Surf-50*hi Depth-2*lo	Surf-5*low for surface Depth-7		S-No Data D-30*high for sub-surf
Chlorophyll concentration chl. conc. ($\mu\text{m L}^{-1}$) (Snow 2006)	>20 μm most dominant size, chl. maximum at surface, high chl conc.	>20 μm most dominant size, chl. maximum at surface, high chl conc.	>20 μm most dominant size, chl. maximum at surface, high chl. conc.	<2 μm most dominant size, chl. maximum at 10-20 m, low chl. conc.	<2 μm most dominant size, chl. maximum at 10-20 m, low chl. conc.	<2 μm most dominant, chl maximum at 10-20 m, low chl. conc.
Iron Growth Rates of phytoplankton (change per hour) (Guo 2006)		>20 μmolL^{-1} conc. showed no effect of iron, growth faster than Bio-4		>20 μmolL^{-1} conc. had positive growth with iron, slowest growth rates		>20 μmolL^{-1} conc. had negative growth with iron, fast growth rate
Zooplankton (Geri 2006)	>333 μm size is dominant	>333 μm size is dominant	>333 μm size is dominant	<333 μm slightly more common	>333 μm size is dominant	<333 μm size is dominant
Amount Zooplankton (Geri 2006)	Bio1>Bio3>Bio6>Bio5>Bio2>Bio4					

Figure 1. Major currents influencing the Galapagos marine ecosystem. These currents are the cause of upwelling that creates the nutrient-rich waters that the diverse marine life depend on to survive.

(<http://www.geol.umd.edu/~jmerck/galsite/research/projects/fitz/currents.gif>)

Figure 2. Areas of high and low chlorophyll concentration around the Galapagos Islands on June 11, 1981 as taken from the Nimbus 7-orbit 13288 (Feldman 1986).

Higher areas of concentration are orange and red, lower areas are blue or green.

Figure 3. Map of High Nutrient- Low Chlorophyll (HNLC) regions around the world, measurement in map is of nitrate, with the scale as a gradient of color pictured on the bottom (<http://www.atmosphere.mpg.de/media/archive/1058.gif>).

Figure 4. Productivity levels around the Galapagos from satellite readings in Feldman (1984). Inset A shows non-El Niño conditions, inset C shows El Niño conditions and inset B shows conditions between the two extremes. Higher areas of concentration are orange and red, lower areas are blue or green. Inset D is a map of the islands showing locations of specific islands

(http://www.atmosphere.mpg.de/enid/0_55a304092d09/2__Oceanic_nutrients/_Iron_in_the_oceans_1vv.html).

Figure 5. Cruise track and Stations in the Galapagos Islands of Ecuador occupied on Leg 2 of cruise TN 189.

Figure 6. SeaWiFS image of chlorophyll concentration on 23 January 2006 during our cruise

(http://oceancolor.gsfc.nasa.gov/cgi/tiles.pl?sub=region_timeseries_table&rqn=GalapagosIs).

Figure 7. Concentration profiles of ammonium (A) and nitrate (B) for all stations. Closed diamonds correspond to Bio-2, closed squares to Bio-2, closed triangles to Bio-3, Xs to Bio-4, open diamonds to Bio-5 and open circles to Bio-6.

Figure 8. Concentration profiles of phosphate (A) and silica (B) for all stations. Closed diamonds correspond to Bio-2, closed squares to Bio-2, closed triangles to Bio-3, Xs to Bio-4, open diamonds to Bio-5 and open circles to Bio-6.

Figure 9. Depth profiles of macronutrient concentrations (A) and CTD data (B) of station Bio-1 (West of Isabela). (A) Square symbols correspond to ammonium data, diamond to nitrate, triangle to phosphate and circles to silica. (B) Solid black line is temperature, dashed black line is salinity, solid grey line is chlorophyll concentration and dashed grey line is dissolved oxygen concentration. Mixed layer depth is about 15 m.

Figure 10. Depth profiles of macronutrient concentrations (A) and CTD data (B) of station Bio-2 (West of Isabela). (A) Square symbols correspond to ammonium data, diamond to nitrate, triangle to phosphate and circles to silica. (B) Solid black line is temperature, dashed black line is salinity, solid grey line is chlorophyll concentration and dashed grey line is dissolved oxygen concentration. Mixed layer depth is about 10 m.

Figure 11. Depth profiles of macronutrient concentrations (A) and CTD data (B) of station Bio-3 (West of Isabela). (A) Square symbols correspond to ammonium data, diamond to nitrate, triangle to phosphate and circles to silica. (B) Solid black line is temperature, dashed black line is salinity, solid grey line is

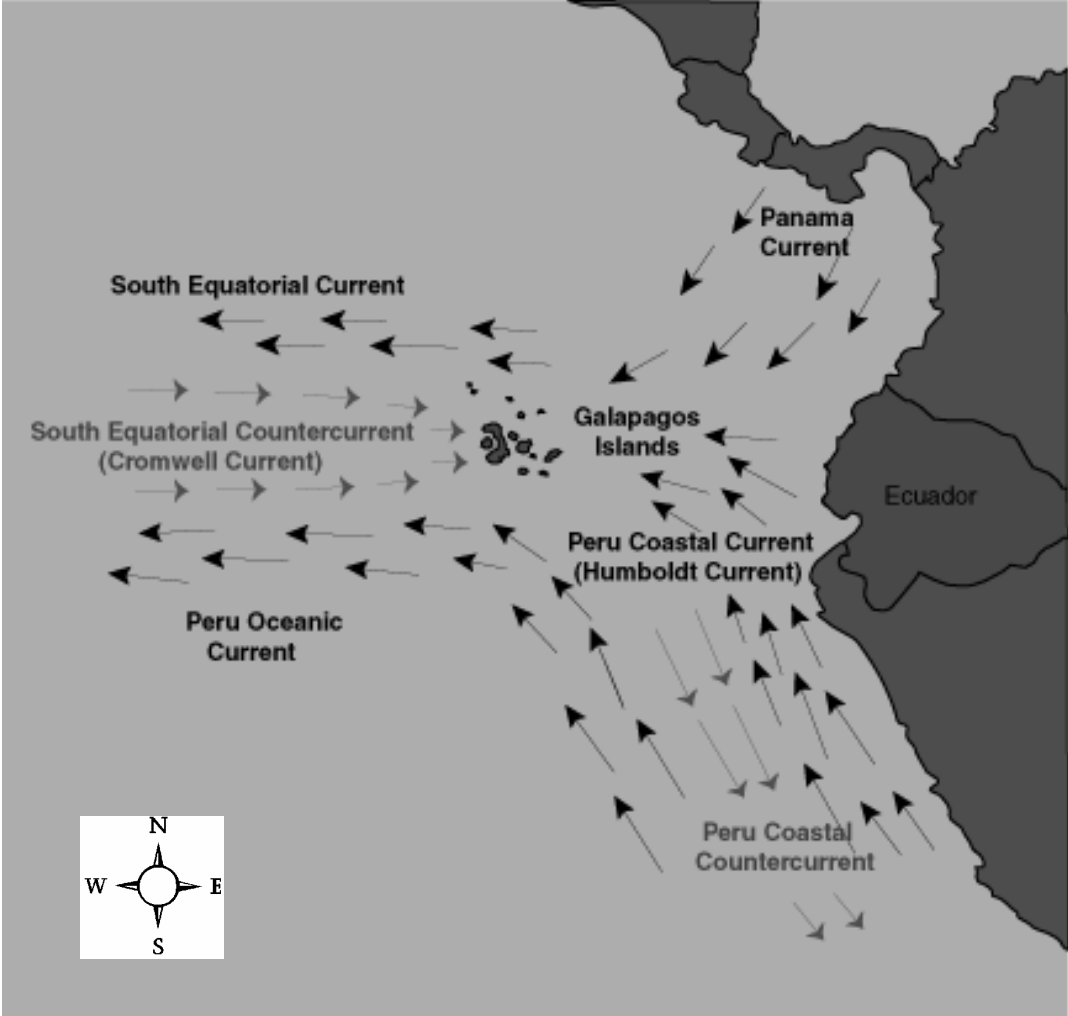
chlorophyll concentration and dashed grey line is dissolved oxygen concentration.
Mixed layer depth is about 10 m.

Figure 12. Depth profiles of macronutrient concentrations (A) and CTD data (B) of station Bio-4 (East of Isabela). (A) Square symbols correspond to ammonium data, diamond to nitrate, triangle to phosphate and circles to silica. (B) Solid black line is temperature, dashed black line is salinity, solid grey line is chlorophyll concentration and dashed grey line is dissolved oxygen concentration. Mixed layer depth is about 25 m.

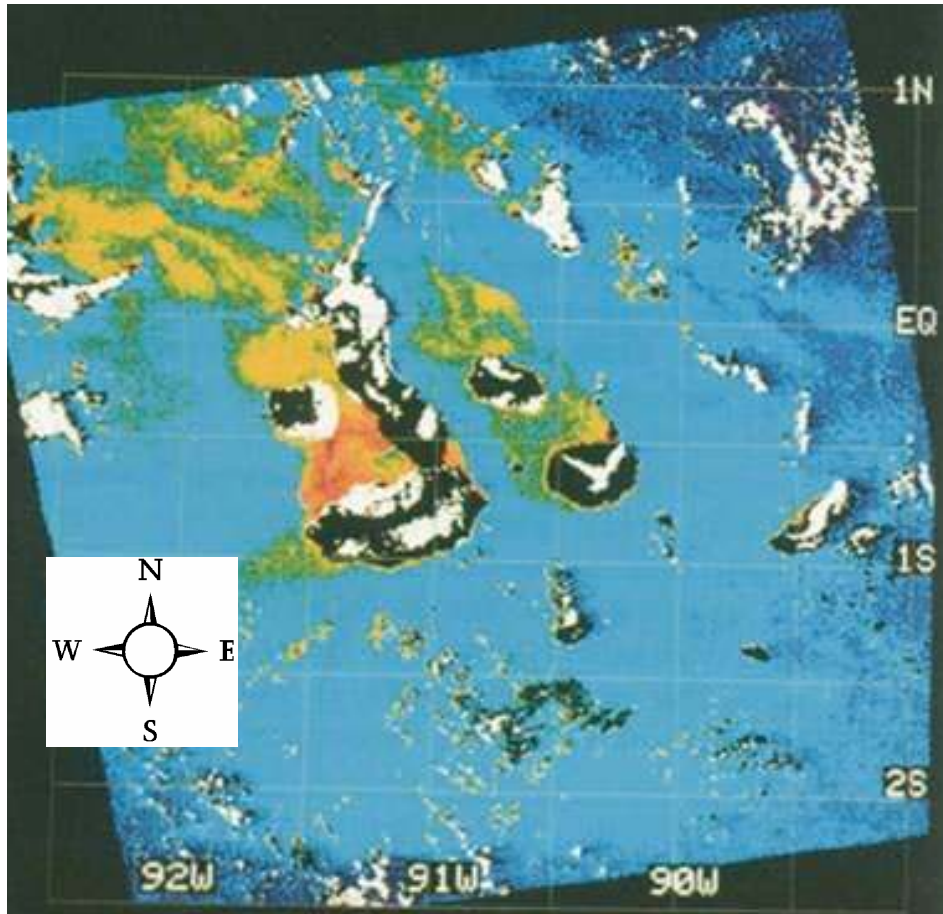
Figure 13. Depth profiles of macronutrient concentrations (A) and CTD data (B) of station Bio-5 (East of Isabela). (A) Square symbols correspond to ammonium data, diamond to nitrate, triangle to phosphate and circles to silica. (B) Solid black line is temperature, dashed black line is salinity, solid grey line is chlorophyll concentration and dashed grey line is dissolved oxygen concentration. Mixed layer depth is about 35 m.

Figure 14. Depth profiles of macronutrient concentrations (A) and CTD data (B) of station Bio-6 (East of Isabela). (A) Square symbols correspond to ammonium data, diamond to nitrate, triangle to phosphate and circles to silica. (B) Solid black line is temperature, dashed black line is salinity, solid grey line is chlorophyll concentration and dashed grey line is dissolved oxygen concentration. Mixed layer depth is about 40 m.

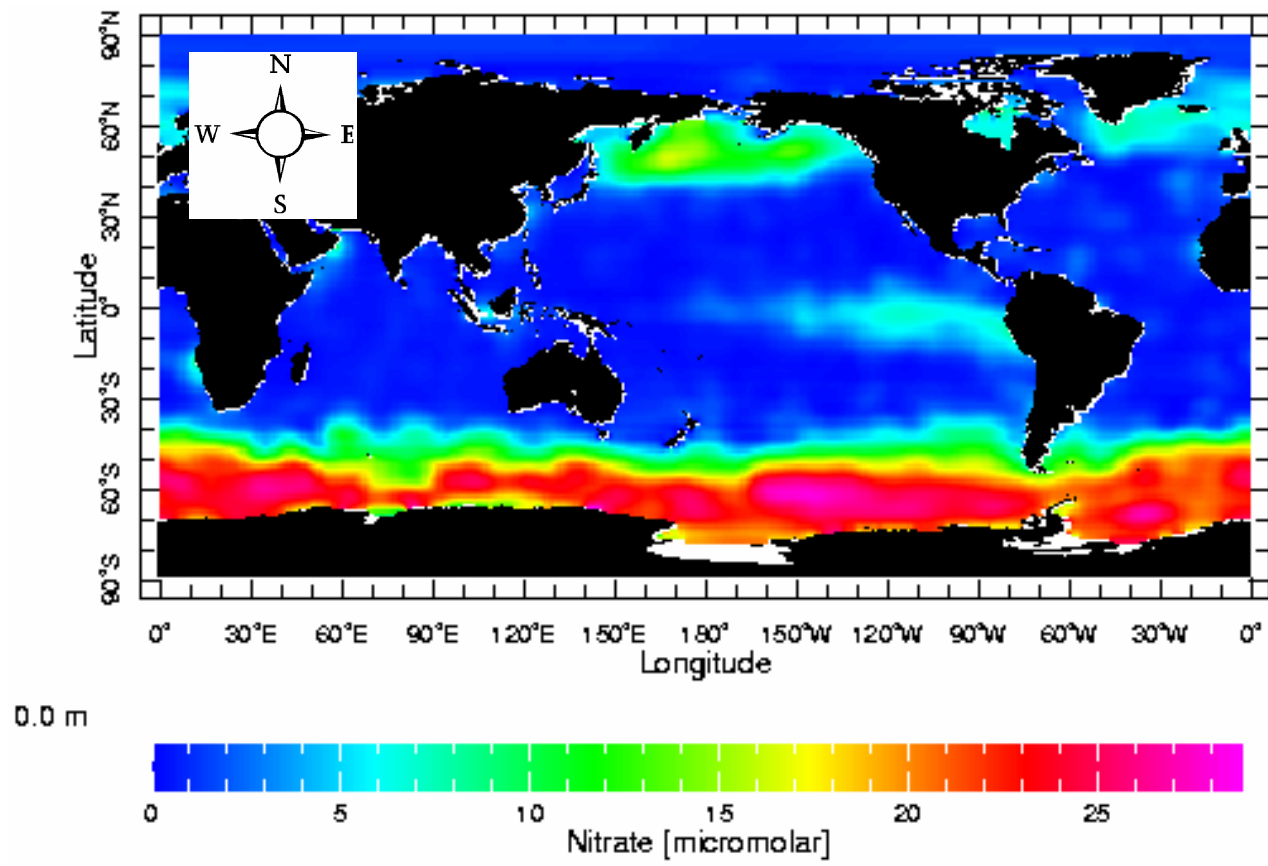
Figure 15. Graph of N:P ratio for all nitrate and phosphate data. Equation of best-fit line through zero is $y = 3.5282x$. The N:P ratio is about 3.5 to 1.



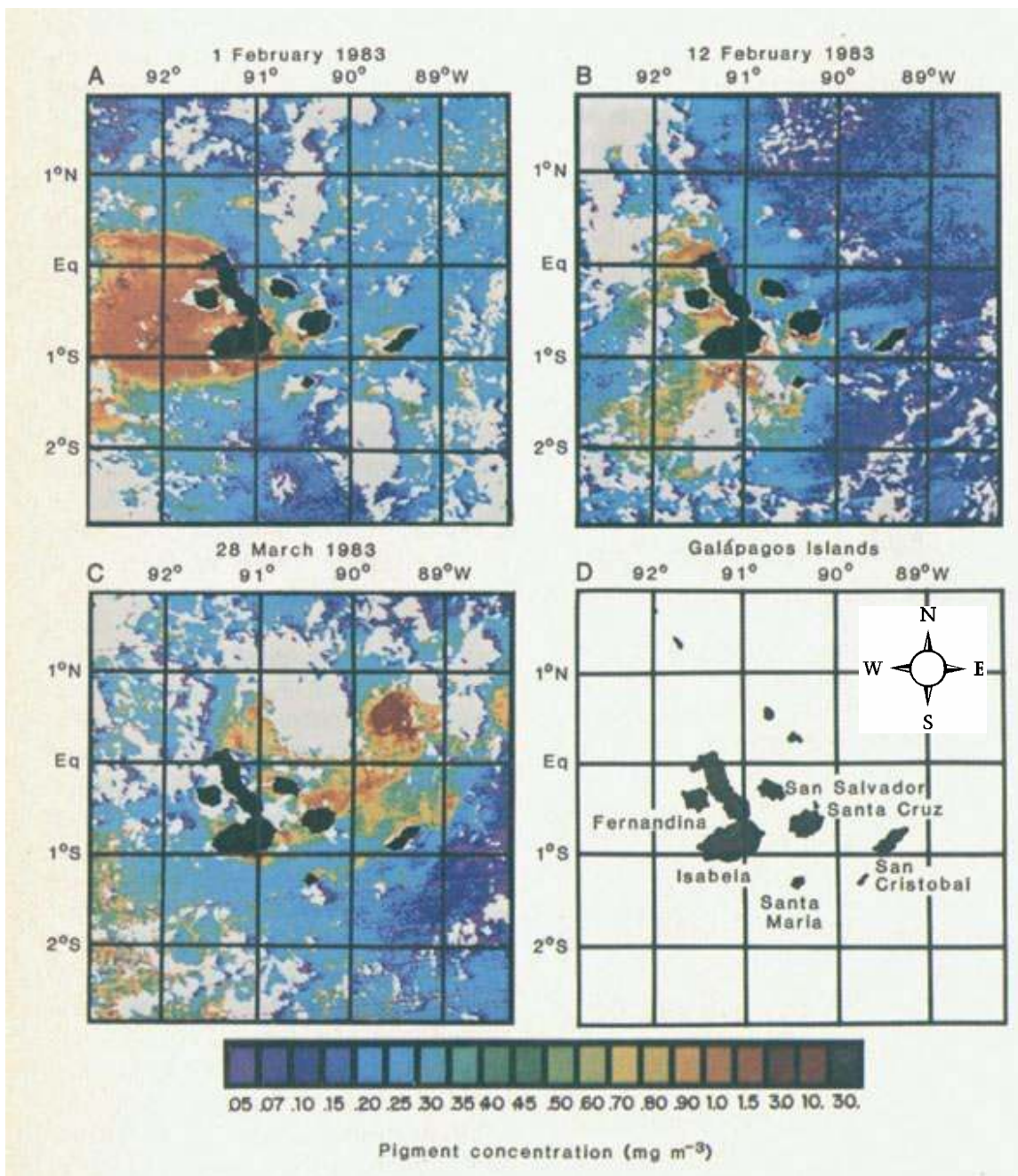
Tamra Dickson Figure 1



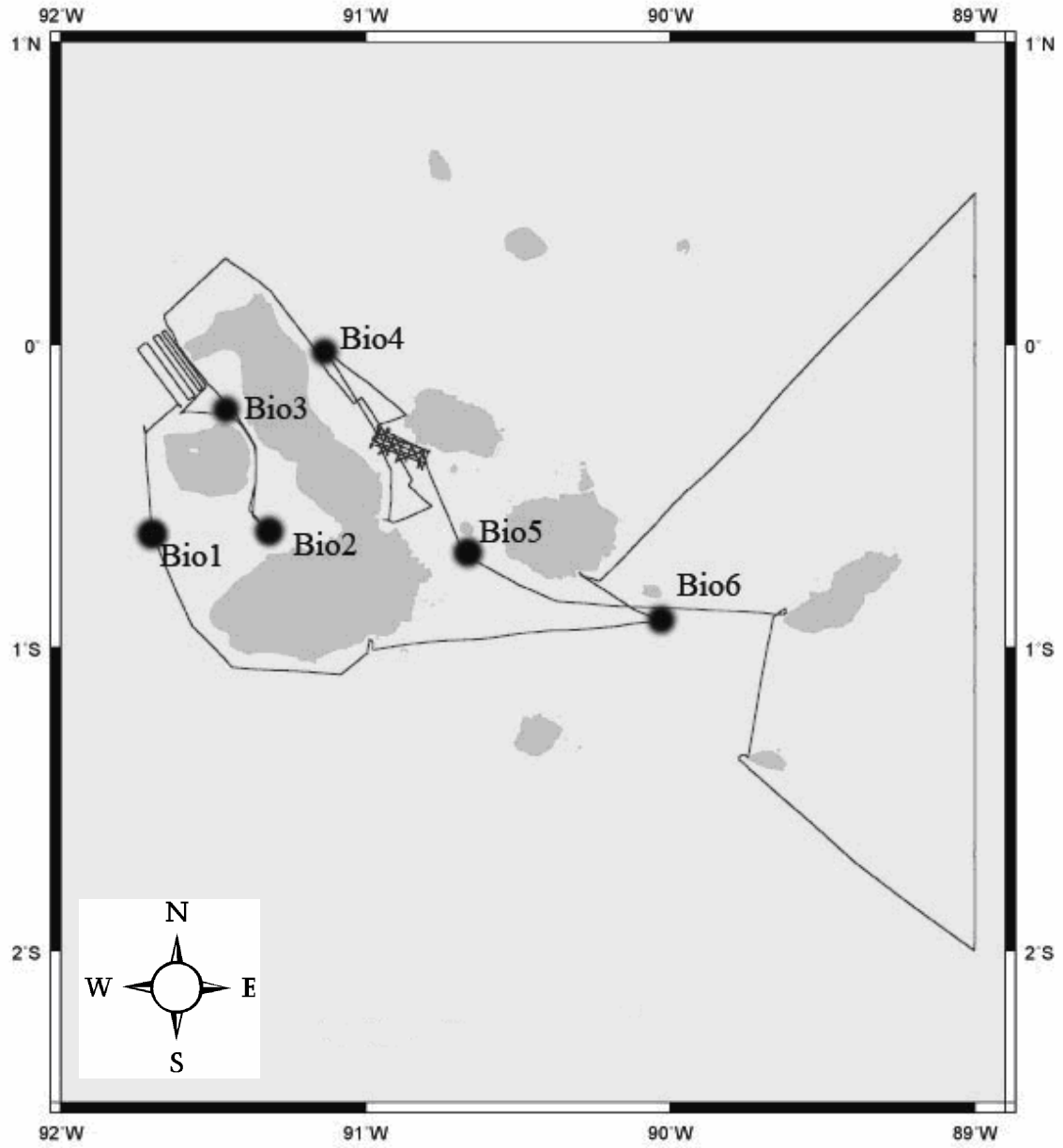
Tamra Dickson Figure 2



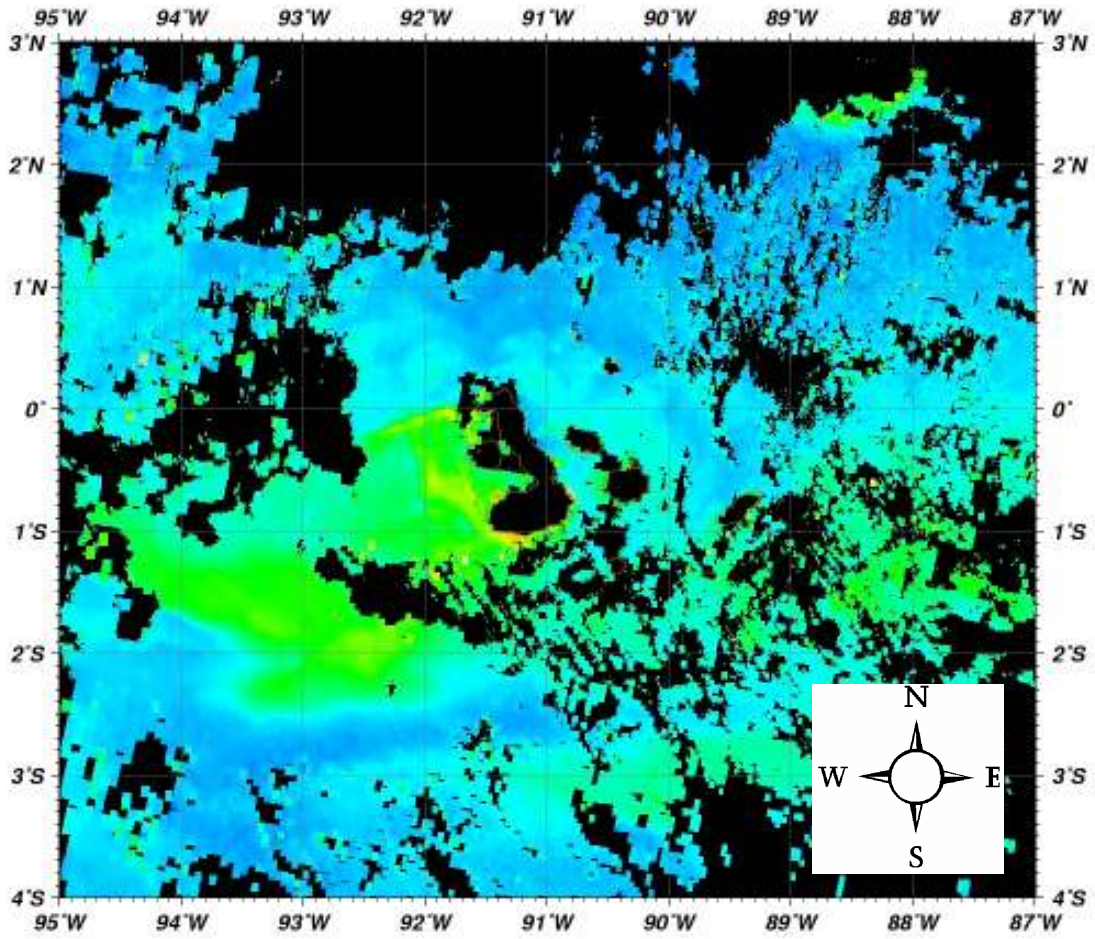
Tamra Dickson Figure 3



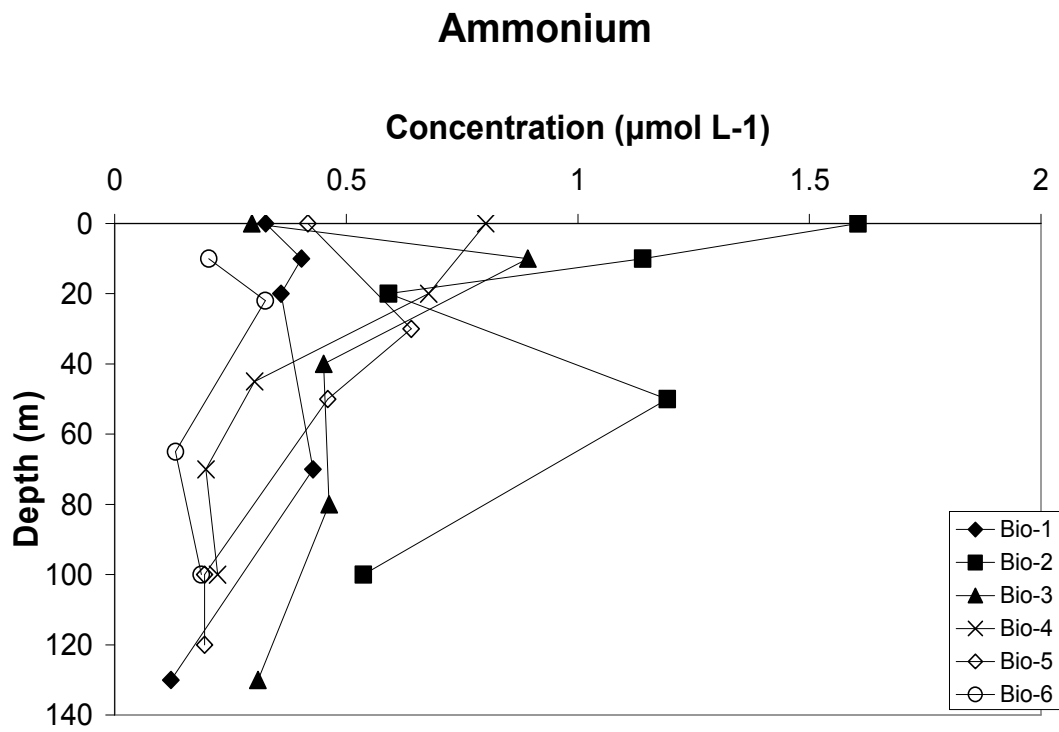
Tamra Dickson Figure 4



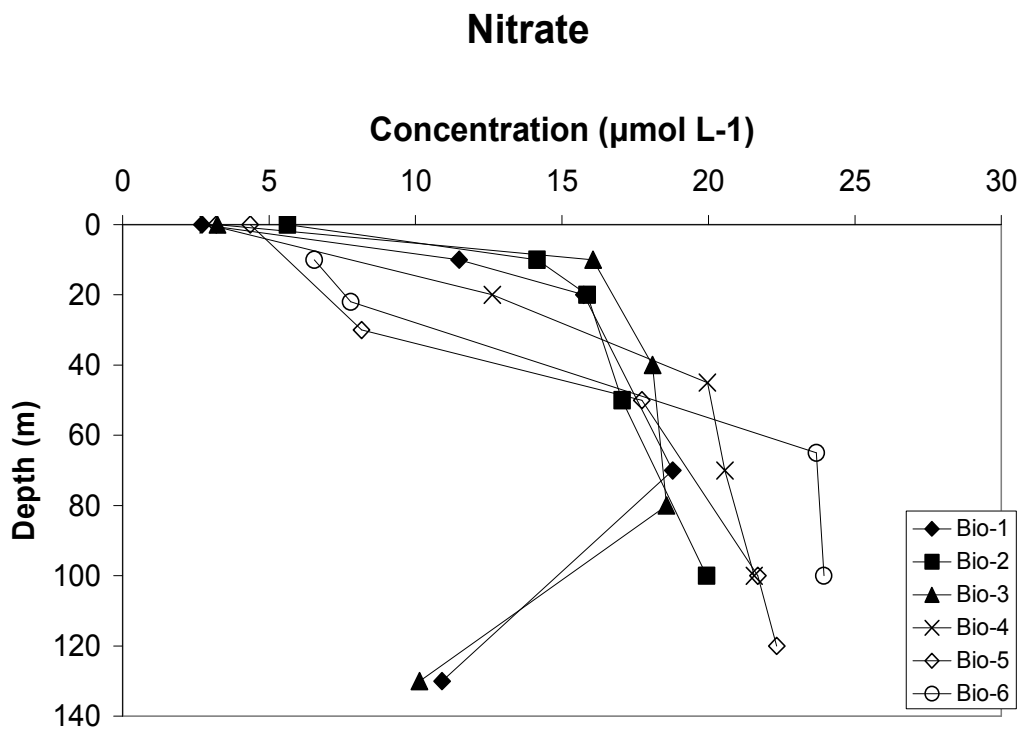
Tamra Dickson Figure 5



Tamra Dickson Figure 6

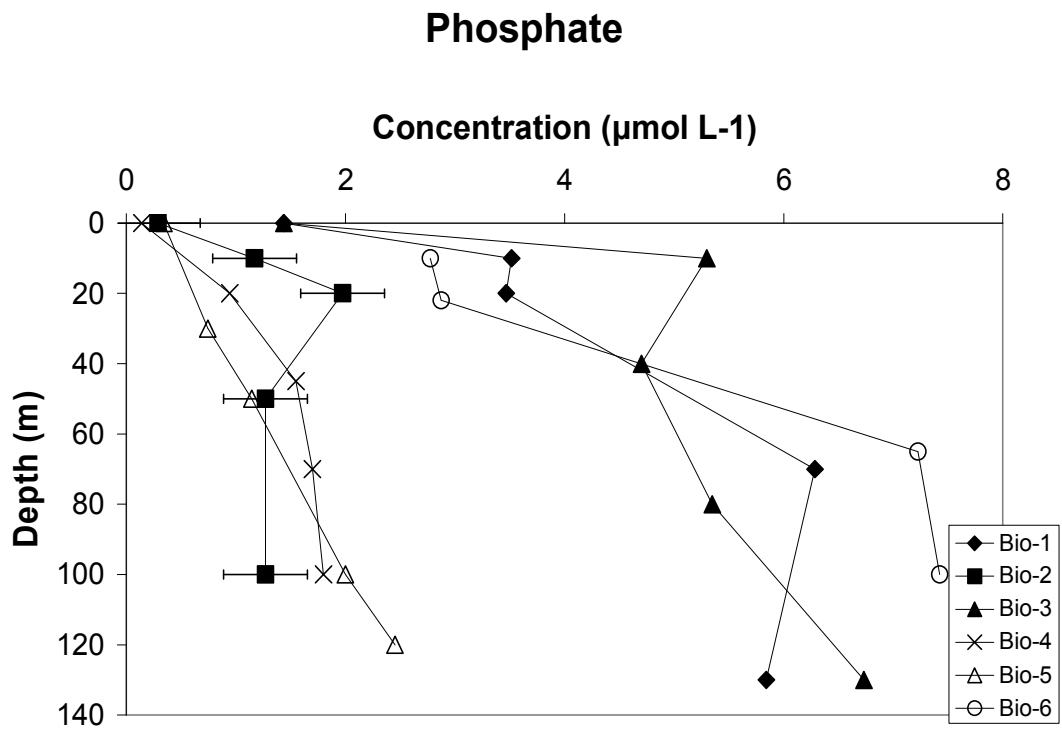


A

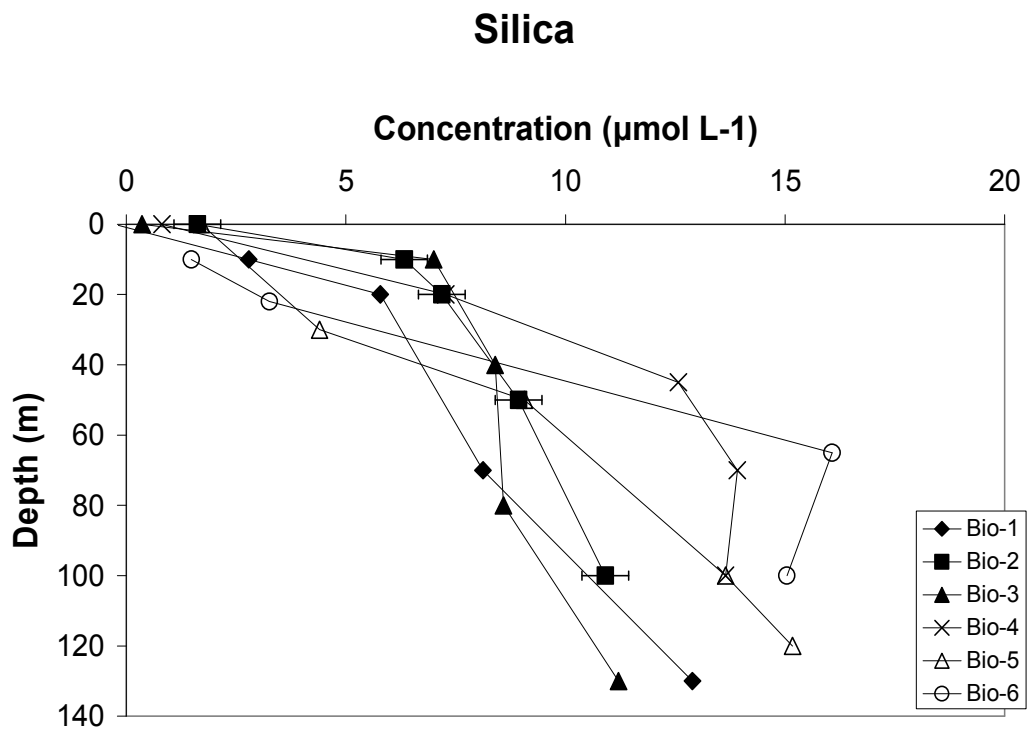


B

Tamra Dickson Figure 7

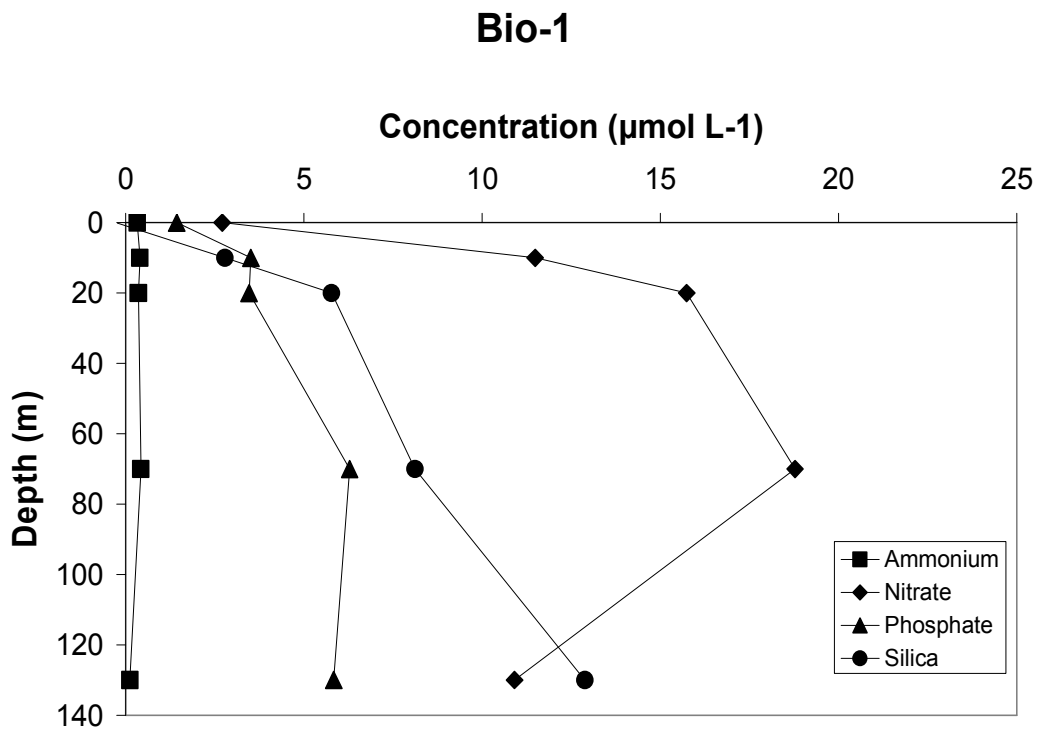


A

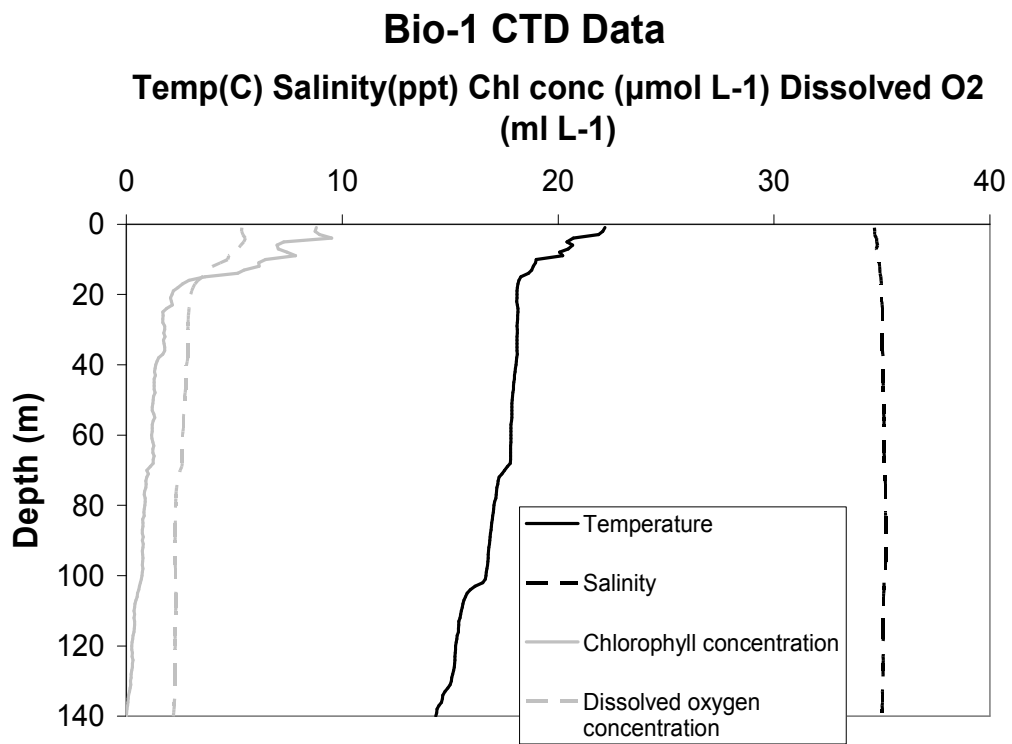


B

Tamra Dickson Figure 8

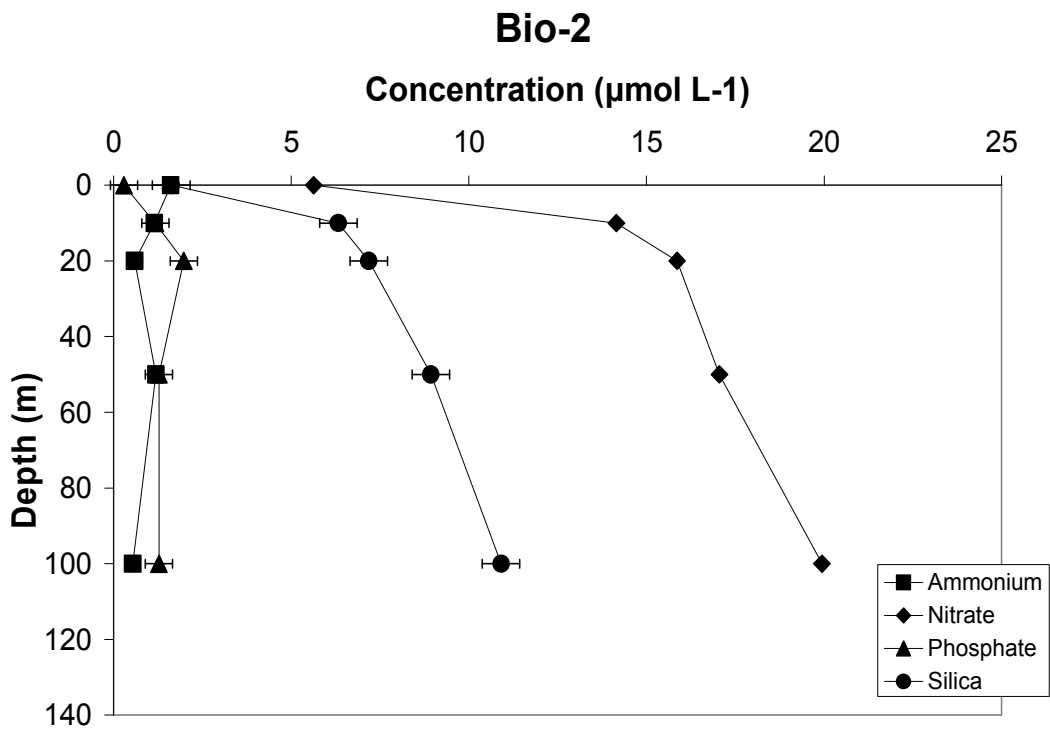


A

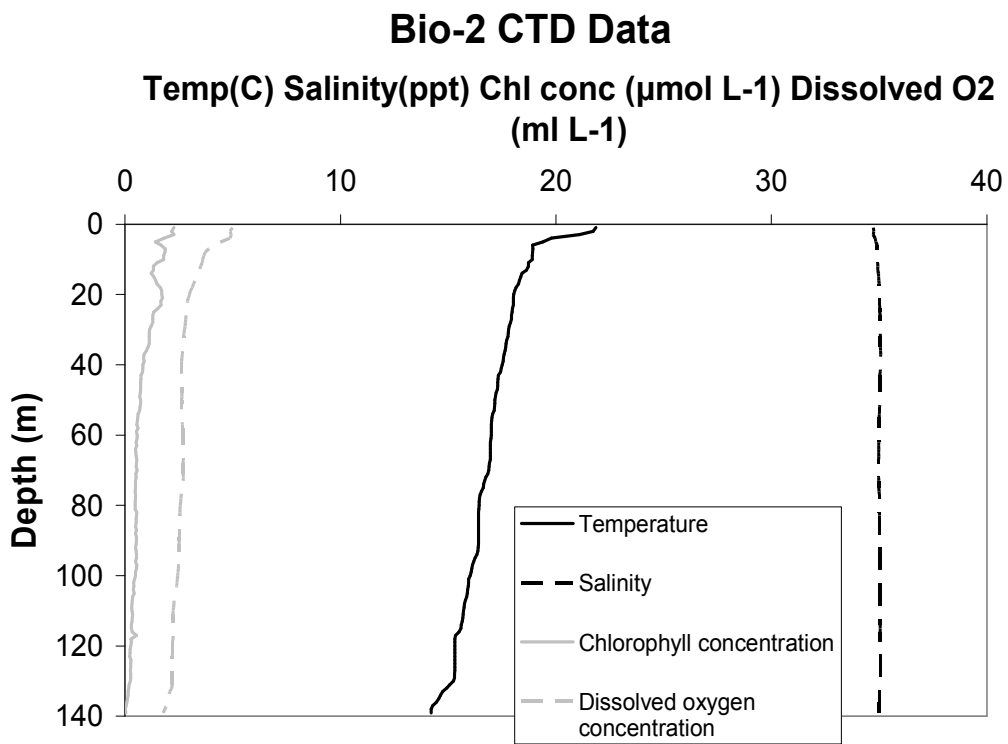


B

Tamra Dickson Figure 9

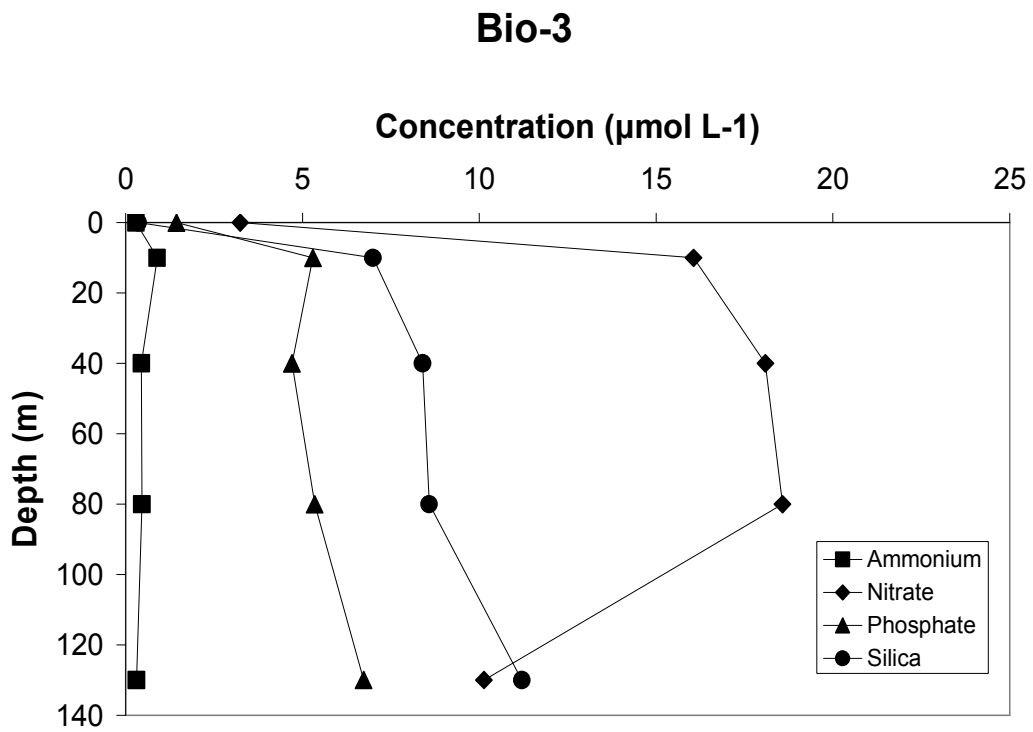


A

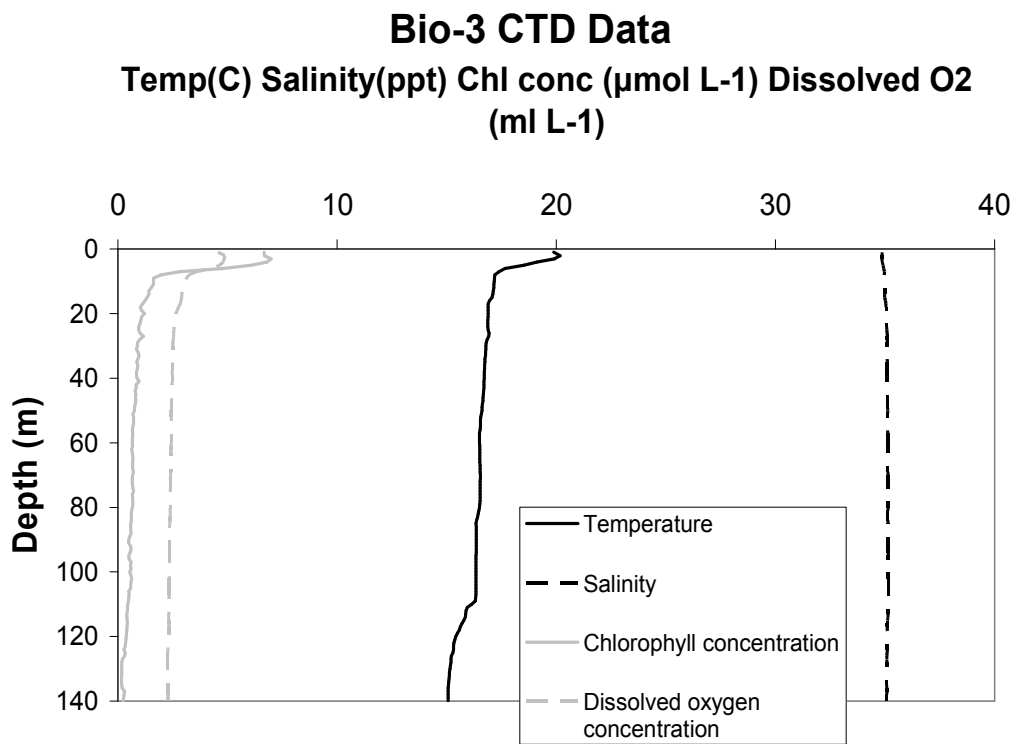


B

Tamra Dickson Figure 10

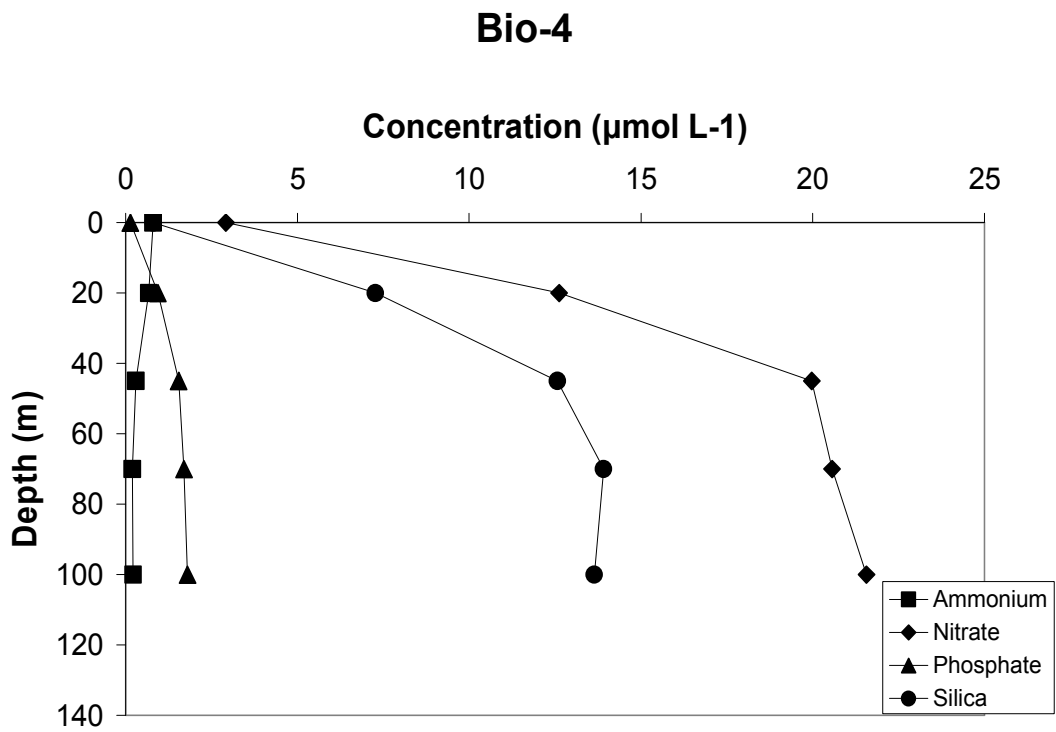


A

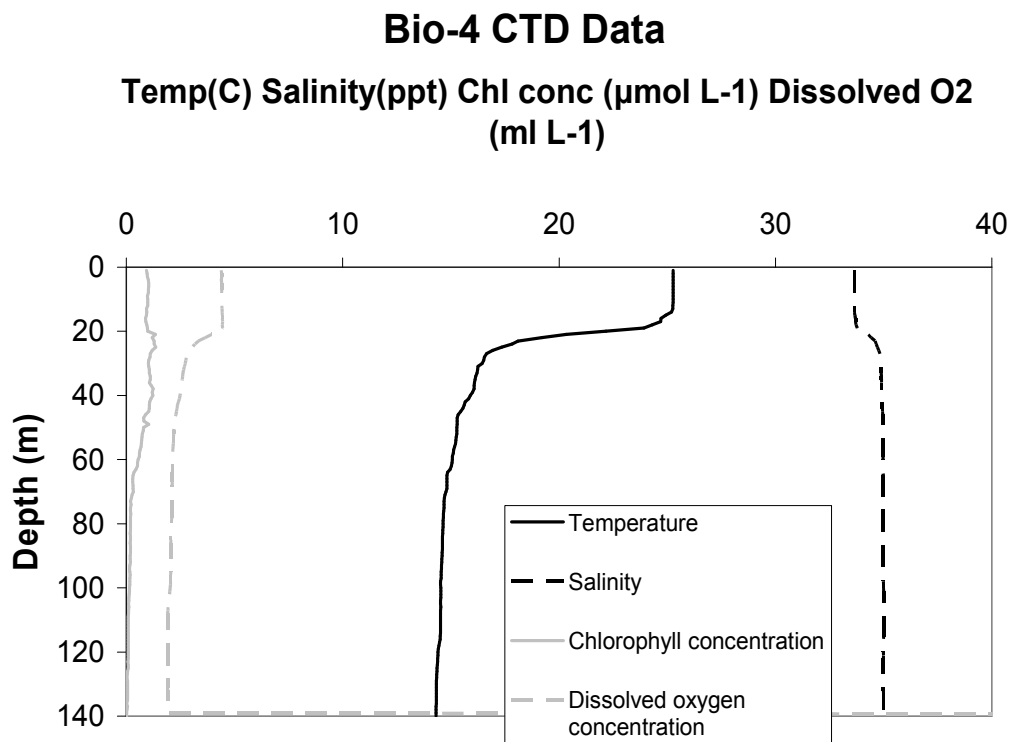


B

Tamra Dickson Figure 11

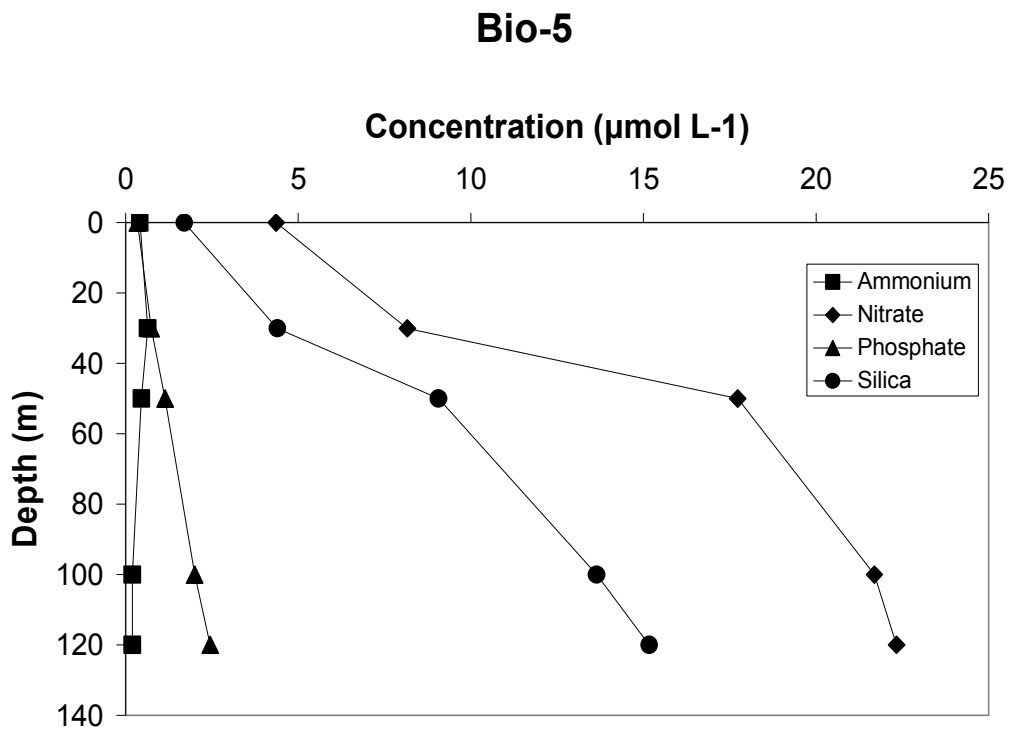


A

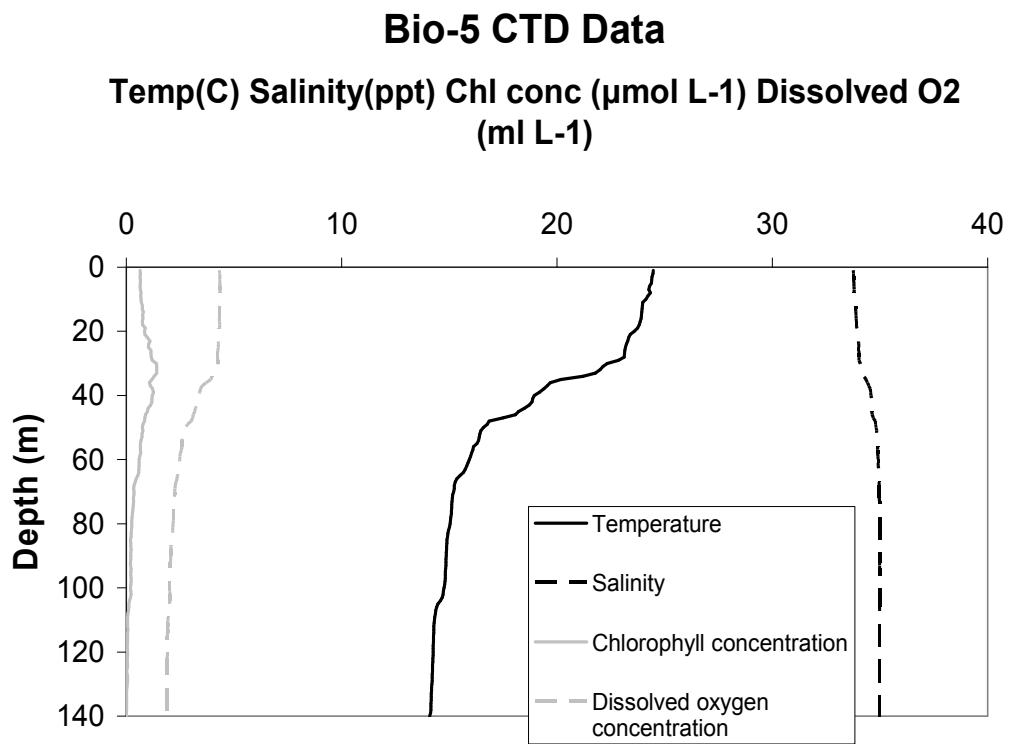


B

Tamra Dickson Figure 12

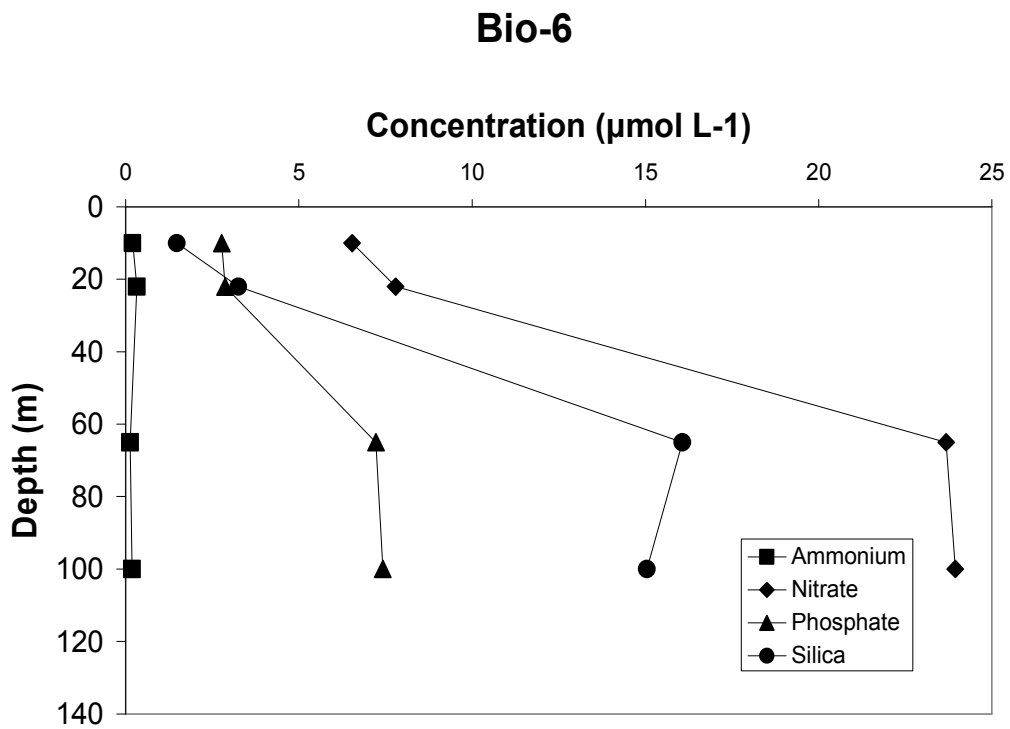


A

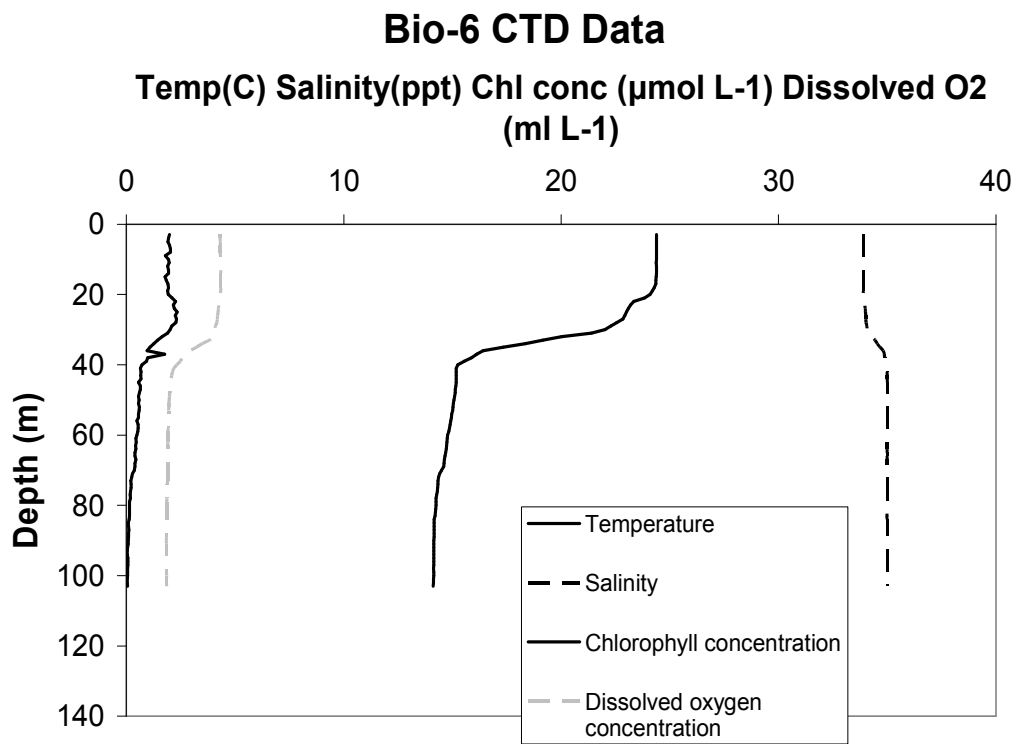


B

Tamra Dickson Figure 13



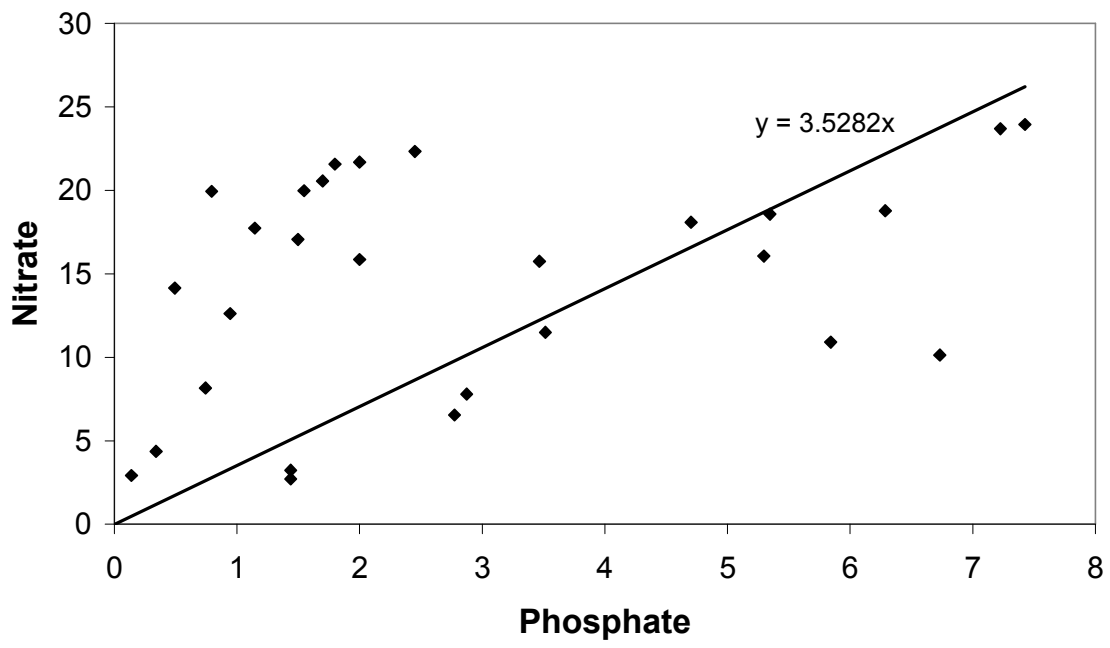
A



B

Tamra Dickson Figure 14

P:N Ratio



Tamra Dickson Figure 15